International Journal of Nanomedicine

Dovepress
open access to scientific and medical research

Open Access Full Text Article

ORIGINAL RESEARCH

Fabrication of ultra-small monolayer graphene quantum dots by pyrolysis of trisodium citrate for fluorescent cell imaging

This article was published in the following Dove Press journal:
International Journal of Nanomedicine

Guo-Lin Hong[1]
Hai-Ling Zhao[2,3]
Hao-Hua Deng[3]
Hui-Jing Yang[4]
Hua-Ping Peng[3]
Yin-Huan Liu[5]
Wei Chen[3]

[1]Department of Laboratory Medicine, The First Affiliated Hospital of Xiamen University, Xiamen 361003, People's Republic of China; [2]School of Public Health, Xiamen University, Xiamen 361102, People's Republic of China; [3]Department of Pharmaceutical Analysis, Higher Educational Key Laboratory for Nano Biomedical Technology of Fujian Province, Fujian Medical University, Fuzhou 350004, People's Republic of China; [4]Department of Laboratory Medicine, Fujian Medical University, Fuzhou 350004, People's Republic of China; [5]Department of Laboratory Medicine, The Affiliated Fuzhou Second Hospital of Xiamen University, Fuzhou 350007, People's Republic of China

Background: The preparation and biological applications of ultra-small graphene quantum dots (GQDs) with accurate-controlled size are of great significance.

Methods: Here in, we report a novel procedure involving pyrolysis of trisodium citrate and subsequent ultrafiltration for fabricating monolayer GQDs with ultra-small lateral size (1.3±0.5 nm).

Results: The GQDs exhibit blue photoluminescence with peak position independent of excitation wavelength. The quantum yield of GQDs is measured to be 3.6%, and the average fluorescence lifetime is 2.78 ns.

Conclusion: Because of high stability and low toxicity, GQDs are demonstrated to be excellent bioimaging agents. The ultra-small GQDs can not only distribute in the cytoplasm but also penetrate into the nuclei. We ensure that this work will add a new dimension to the application of graphene materials for nanomedicine.

Keywords: graphene quantum dots, fluorescence, cell imaging, trisodium citrate, pyrolysis

Introduction

Graphene quantum dots (GQDs), a new kind of nanomaterial with the combined properties of graphene and quantum dots, are graphene sheets with lateral dimensions less than 100 nm in single-, double- and few-layer.[1–5] As zero dimensional carbon nanomaterials, GQDs have shown numerous wonderful physical and chemical properties due to the pronounced quantum confinement and edge effects.[6–8] Compared with organic dyes and semiconductive quantum dots, GQDs are superior in terms of high specific surface area, high photostability against photobleaching and blinking, excellent biocompatibility, and low toxicity.[4] In addition, the graphene structure inherent in GQDs endows them with some of the unusual properties of graphene. For these reason, GQDs are proposed to be applicable in various fields, such as biological imaging,[9–11] sensing,[12] drug delivery,[13] catalysis,[14,15] and photovoltaics.[16]

The strategies for the preparation of GQDs can be divided into two major categories: top-down and bottom-up approaches. The top-down splitting method involves exfoliating or breaking down of carbonaceous materials, such as soot, coal, carbon black, graphene, graphene oxide, carbon nanotubes, and carbon fibers, through hydrothermal, electrochemical, concentrated acid oxidation, and microwave or ultrasonic exfoliation methods.[17–25] These methods lack precise control of the morphology and size distribution of the products, what's more, they sometimes require special instruments to operate. The bottom-up organic approach, however, is realized by pyrolysis or carbonization of small organic molecules or by step-wise chemical fusion of small aromatic

Correspondence: Wei Chen
Department of Pharmaceutical Analysis, Higher Educational Key Laboratory for Nano Biomedical Technology of Fujian Province, Fujian Medical University, Fuzhou 350004, People's Republic of China
Tel/fax +86 591 2286 2016
Email chenandhu@163.com

submit your manuscript | www.dovepress.com
Dovepress
http://dx.doi.org/10.2147/IJN.S168570

structures molecules.[26–30] These methods allow for excellent control of the properties of the final product.

One of the major areas where GQDs have been used in the biological and health sciences is bioimaging.[31] Their intrinsic luminescence offers a very inexpensive option as probes to visualize biological matter both in vivo and in vitro. There have been varying reports on cell imaging based on GQDs with different luminescence and lateral size (>2 nm).[11,22,24,27,32–34] In these cases, GQDs accumulate mainly in the cytoplasm of cells, but minimally in the nucleus. Cellular uptake and distribution of GQDs have been found to be related to their lateral size.[35] Therefore, the preparation and biological applications of ultra-small GQDs with accurate-controlled size are of great significance. Herein, we report a new bottom-up route toward the synthesis of blue-photoluminescent GQDs. The synthesis procedure is simple and fast. Trisodium citrate, which is easily obtained, is directly used as the organic precursor. Monolayer GQDs with ultra-small lateral size (1.3±0.5 nm) were obtained via ultrafiltration. Due to their stable photoluminescence and low cytotoxicity, the GQDs are demonstrated to be excellent probes for cell imaging. The ultra-small monolayer GQDs can not only distribute in the cytoplasm but also penetrate into the nuclei.

Materials and methods

Chemicals and materials

Trisodium citrate dihydrate and dimethyl sulfoxide (DMSO) were purchased from Sinopharm Chemical Reagent Co., Ltd (Shanghai, People's Republic of China). 3-(4,5-dimethylthiazol-2-yl)–2,5-diphenyl tetrazolium bromide (MTT) and trypsin were bought from Sigma-Aldrich (St Louis, MO, USA). Dulbecco's Modified Eagle's Medium (DMEM) was bought from Haikelong Biochemical Products Co., Ltd (Peking, People's Republic of China). Fetal bovine serum (FBS) was bought from Life Technologies Co., Ltd (Thermo Fisher Scientific, Waltham, MA, USA). Phosphate-buffered saline (PBS) was bought from Kenuo Biotechnology Co., Ltd (Fuzhou, People's Republic of China). Ultrapure water was used throughout. Unless specified, all other chemicals were of at least analytical reagent grade and used without any further purification.

Preparation of GQDs

GQDs were synthesized by pyrolyzing trisodium citrate. In a typical procedure, 0.5 g trisodium citrate was directly heated at 200°C for 4 minutes. The white powder turned to deep brown, which implied the formation of GQDs. Then, 6 mL water was added drop by drop into pre-GQDs, followed by vigorous stirring for 10 minutes to get a colloidal solution. The solution was further ultrafiltered in-turn through centrifugal filter devices with a cutoff molecular weight of 10 and 3 kDa. The product with molecular weight of 3~10 kDa was collected for further characterization and use.

Characterization of GQDs

The size and morphology of GQDs was analyzed by using a JEM 2100F transmission electron microscope at an operating voltage of 200 KV. The height distribution of the GQDs was characterized by atomic force microscope (AFM) (Bruker Multimode, Bruker Corporation, Billerica, MA, USA) operating in tapping mode. The X-ray diffraction (XRD) pattern was measured using a Bruker-D8 Advance (Bruker Corporation) and Cu Kα radiation (λ=1.54051 Å) operating at 1 KV. The Fourier transform infrared spectroscopy (FTIR) spectra were measured by a Nicolet iS5 FT-IR (Thermo Nicolet, Thermo Fisher Scientific) spectrometer with the KBr pellet technique. X-ray photoelectron spectroscopy (XPS) was performed using a Thermo Scientific Escalab 250Xi with Al Kα X-ray radiation as the X-ray source for excitation. Binding energies were corrected using the C1s peak at 284.6 eV as the standard. PL spectra of GQDs were recorded using a Cary Eclipse fluorescence spectrophotometer (Agilent Technologies, Santa Clara, CA, USA). The fluorescence lifetime was measured using a photo-counting HORIBA FL-4 system, with a diode laser emitting at 330 nm as the light source.

In vitro cytotoxicity evaluation

The cytotoxicity of GQDs was evaluated by an MTT assay. The human cell lines HeLa were purchased from the Cell Bank of Shanghai Institute of Biochemistry and Cell Biology, Chinese Academy of Sciences (Shanghai, China). HeLa cells were seeded in a 96-well plate at a density of 5×10^3 cells per well and cultured in Dulbecco's Modified Eagle's Medium (DMEM) with 10% fetal bovine serum (FBS) for 12 hours. Then the cells were incubated with GQDs with different concentrations. After 24 hours, the wells were washed with PBS (pH 7.4), and 200 μL of freshly prepared MTT (0.5 mg/mL) solution was added to each well. The MTT medium solution was removed after 4 hours incubation. 150 μL DMSO was added into each well, and the plate was gently shaken for 30 minutes at room temperature to dissolve all precipitates formed. The absorbance of MTT at 570 nm was recorded by the microplate reader (Thermo Fisher Scientific). Cell viability was expressed by the ratio of absorbance of the cells incubated with GQDs to that of the cells incubated with culture medium only.

Cellular imaging

HeLa cells were maintained in the DMEM supplemented with 10% FBS in 5% CO_2 at 37°C. When the cells were grown to the density of 80% confluence, the medium was removed and the adherent cells were washed twice with PBS buffer (pH 7.4). The GQDs solution was then added to the chamber. After incubation for 2 hours, cells were washed with PBS (pH 7.4) and then imaged by a fluorescence microscope (LEICA DMI3000B).

Results and discussion

Characterization of the morphology and composites of the GQDs

As shown in Scheme 1, the GQDs were synthesized based on pyrolysis of the precursor trisodium citrate and purification by two-stage ultrafiltration. The morphology of the obtained GQDs was characterized by transmission electron microscopy (TEM) and atomic force microscopy (AFM). As shown in Figure 1A, the GQDs are monodispersed and uniformly distributed without apparent agglomeration. The average diameter of the GQDs was 1.3±0.5 nm according to the statistical calculation of more than 200 dots (Figure 1B). They are distinct from other GQDs prepared by bottom-up method, which have relatively large diameter and wide size distribution.[26,28,30,32,36] They are also desirably smaller than most macromolecules in a cell. The inset HRTEM image shows high crystallinity of the GQDs and displays a continuous lattice spacing of 0.22 nm, which corresponds to (1120) lattice fringes of graphite.[37] Furthermore, the ordered carbon hexagon structures have been readily observed, which implies that the GQDs consist of intact sp2 clusters. The AFM image reveals that the topographic height of the GQD is ~0.6 nm, in good agreement with the thickness of single-layer graphene (Figure 1C).[36] To confirm the formation of GQDs, XRD patterns were used to characterize the precursor and the product. As shown in Figure 1D, the XRD pattern of trisodium citrate exhibited a series of sharp peaks, indicating that sodium citrate is of high crystallinity. The pyrolysis products had an obvious diffraction peak at 23.07°, suggesting that carbonizing trisodium citrate would produce graphene structures. The peak is broad due to the small size of the GQDs.

The detailed elemental compositions and functional groups of the GQDs were characterized using XPS and FTIR. As shown in Figure 2A, the GQDs are mainly composed of C, O, Na and H. The high-resolution spectrum of C1s could be deconvoluted into three surface components, corresponding to C=C/C–C (283.6 eV), C–O (285.2 eV), and C=O (287.1 eV), respectively (Figure 2B). The high-resolution spectrum of O1s confirmed the presence of C=O (530.3 eV), C–OH (531.9 eV), and O=C–OH (535.1 eV) bonds (Figure 2C). As shown in the FTIR spectrum (Figure 2D), the absorption peaks centered at 1,402 and 1,591 cm^{-1} are attributed to the symmetric and antisymmetric vibrations of COO^-, respectively. The broad absorption peak centered at 3,428 cm^{-1} is attributed to O–H stretching vibration. It should be noted that the GQDs exhibit nearly no absorption of C–H and C–O–C, implying that they have few surface defects and main functional group of carboxyl on the edge.[28,38] These oxygen-containing functional groups make GQDs soluble in aqueous medium. Even stored for 3 months, there is no precipitation.

Fluorescence properties of the GQDs

Luminescence property is one of the important features of GQDs. The GQDs aqueous solution was pale-brown under visible light and showed naked-eye observable blue fluorescence under 302 nm UV lamp irradiation (Figure 3A). As compared with the GQDs prepared by citric acid as the precursor, the GQDs produced by the pyrolysis of sodium citrate had a blue-shifted fluorescence emission peak at 420 nm, corresponding to their smaller size.[28,39] Furthermore, excitation-independent fluorescence emission curves were observed (Figure S1), implying that both the size and the surface state of those sp2 clusters contained in GQDs should be uniform.

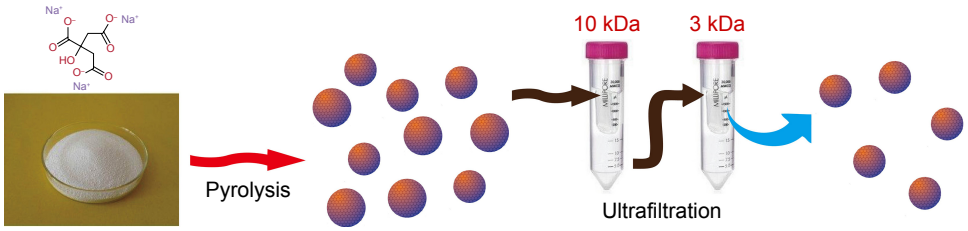

Scheme 1 Processing diagram for the preparation of photoluminescent GQDs.
Abbreviation: GQDs, graphene quantum dots.

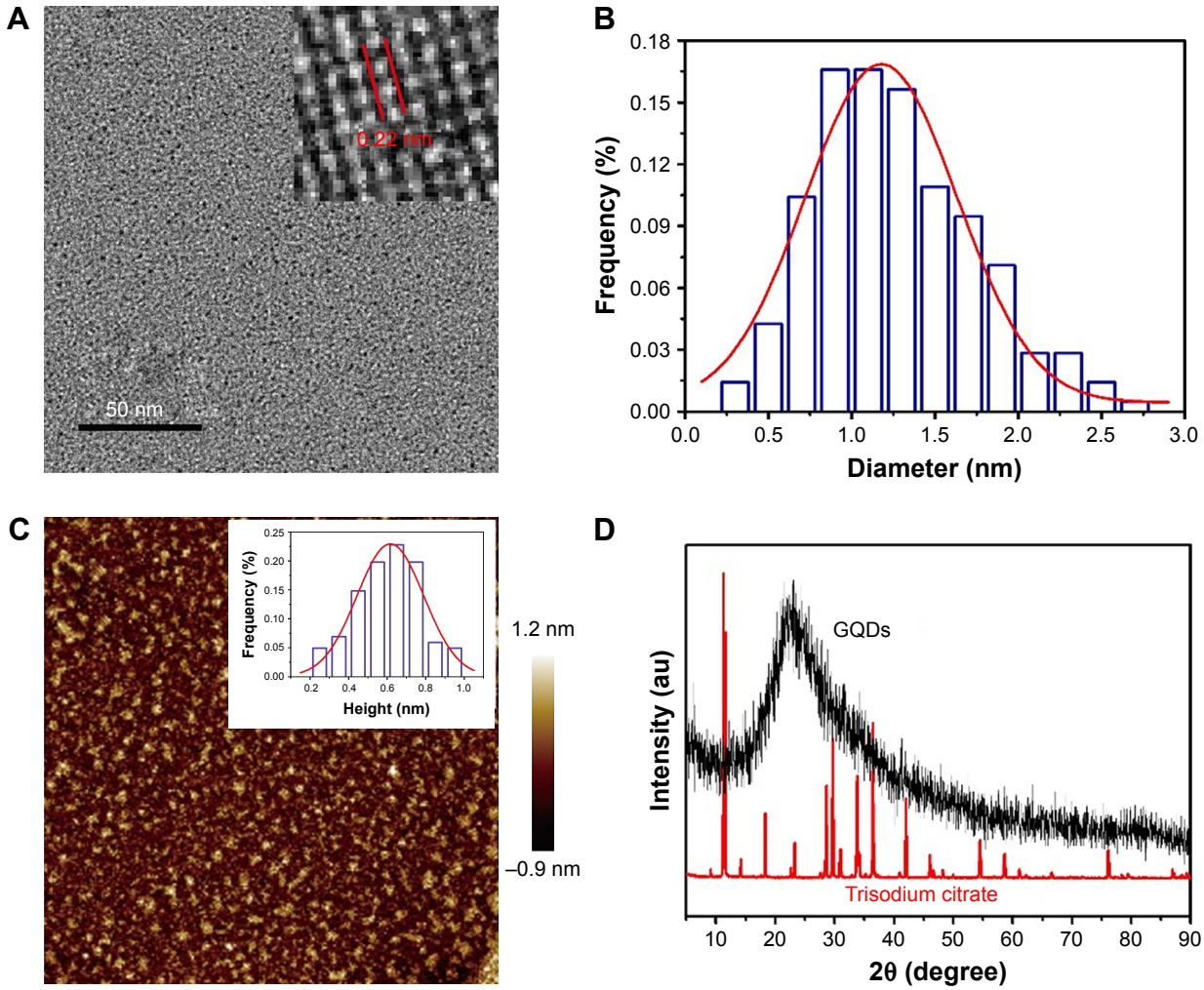

Figure 1 (**A**) The TEM image of GQDs. Inset: a typical single GQD with a lattice spacing of 0.22 nm. (**B**) The size distribution of GQDs calculated from 200 dots. (**C**) AFM image of GQDs. Inset: the height distribution of the GQDs calculated from 100 dots as shown in the AFM image. (**D**) XRD pattern of trisodium citrate and GQDs.
Abbreviations: TEM, transmission electron microscopy; GQDs, graphene quantum dots; AFM, atomic force microscopy; XRD, X-ray diffraction.

Using quinine sulfate as a reference dye the quantum yield of GQDs was measured to be 3.6% with excitation at 330 nm. The fluorescence lifetime curve of GQDs at 420 nm emission wavelength with 330 nm excitation is shown in Figure 3B. The fluorescence emission exhibited well fitted triple-exponential function. The average fluorescence lifetime was 2.78 ns. The nanosecond lifetime shows the potential applications of GQDs in optoelectronics and biological analysis.

In order to further understand the characteristics of the GQDs, we investigated their fluorescence stability under different conditions. As shown in Figure 4A, the GQDs had good salt tolerance. Even in the presence of 2 M NaCl, the fluorescence intensity could still retain its original value. Figure 4B shows the effect of pH value on the fluorescence of GQDs. It was found that the fluorescence intensity of GQDs increased with the increase of the pH value in acidic pH range 3.0–5.5, which could be ascribed to protonation and deprotonation of the carboxyl groups on the surface of the GQDs. In neutral and alkaline pH range 5.5–11.0, the fluorescence intensity of GQDs was almost kept unchanged. It is worth noting that the GQDs exhibited >60% fluorescence intensity retention when the pH value of the solution was higher than 3.0, implying a great potential application in various pH conditions. Figure 4C shows that GQDs also had excellent thermal stability. The fluorescence intensity could be maintained above 94% when the solution was heated to 90°C. The fluorescence of GQDs remained almost unchanged at room temperature for more than 3 months (Figure 4D). Compared to traditional organic dyes, such as FITC, the GQDs had good photostability. As shown in Figure 4E, the GQDs maintained a stable fluorescence emission when exposed to the ultraviolet light (330 nm) for a long time. This photobleaching resistance feature provides

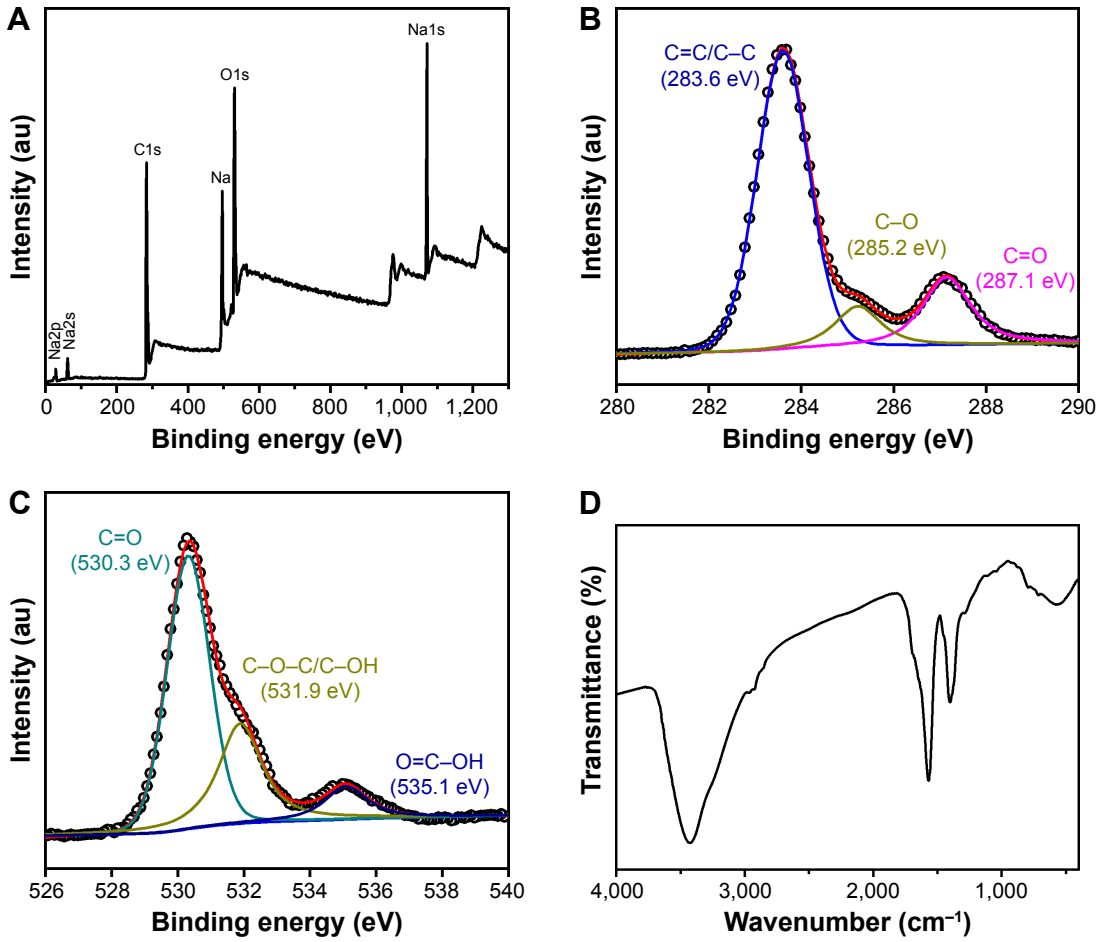

Figure 2 (**A**) XPS survey spectrum of the GQDs. (**B**) XPS high-resolution spectrum of C1s core levels in the GQDs. (**C**) XPS high-resolution spectrum of O1s core levels in the GQDs. (**D**) FTIR spectrum of the GQDs.
Abbreviations: XPS, X-ray photoelectron spectroscopy; GQD, graphene quantum dots; FTIR, Fourier transform infrared spectroscopy.

the GQDs with great potential for in vitro and in vivo fluorescence imaging applications. We further investigated the effect of hydrogen peroxide, a common reactive oxygen species in biological systems, on the fluorescence of GQDs. As shown in Figure 4F, although high concentration of hydrogen peroxide quenched the fluorescence, the hydrogen peroxide less than 10 mM did not affect the fluorescence intensity of GQDs.

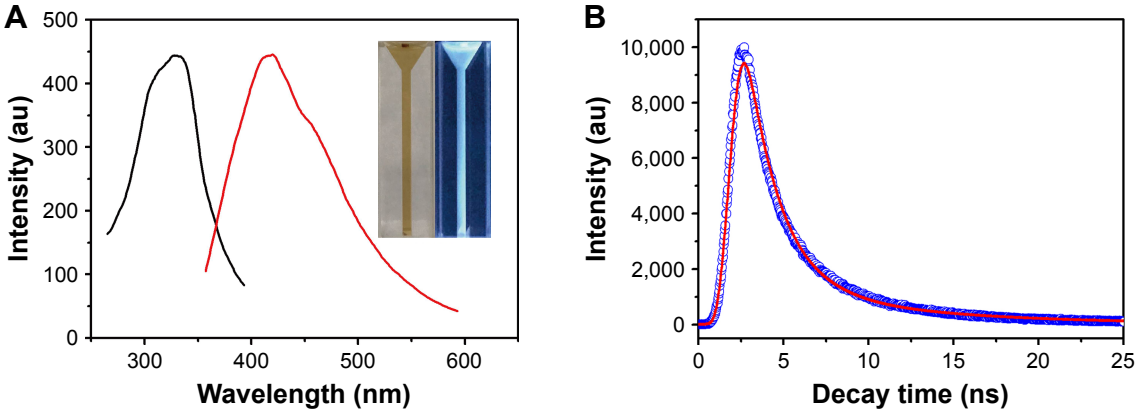

Figure 3 (**A**) PL and PLE spectra of the GQDs. The insert shows the photographs of the GQDs aqueous solution under visible light and 302 nm UV light. (**B**) PL decay curve at 420 nm for the GQDs.
Abbreviations: PL, photoluminescence; PLE, photoluminescence excitation; GQDs, graphene quantum dots.

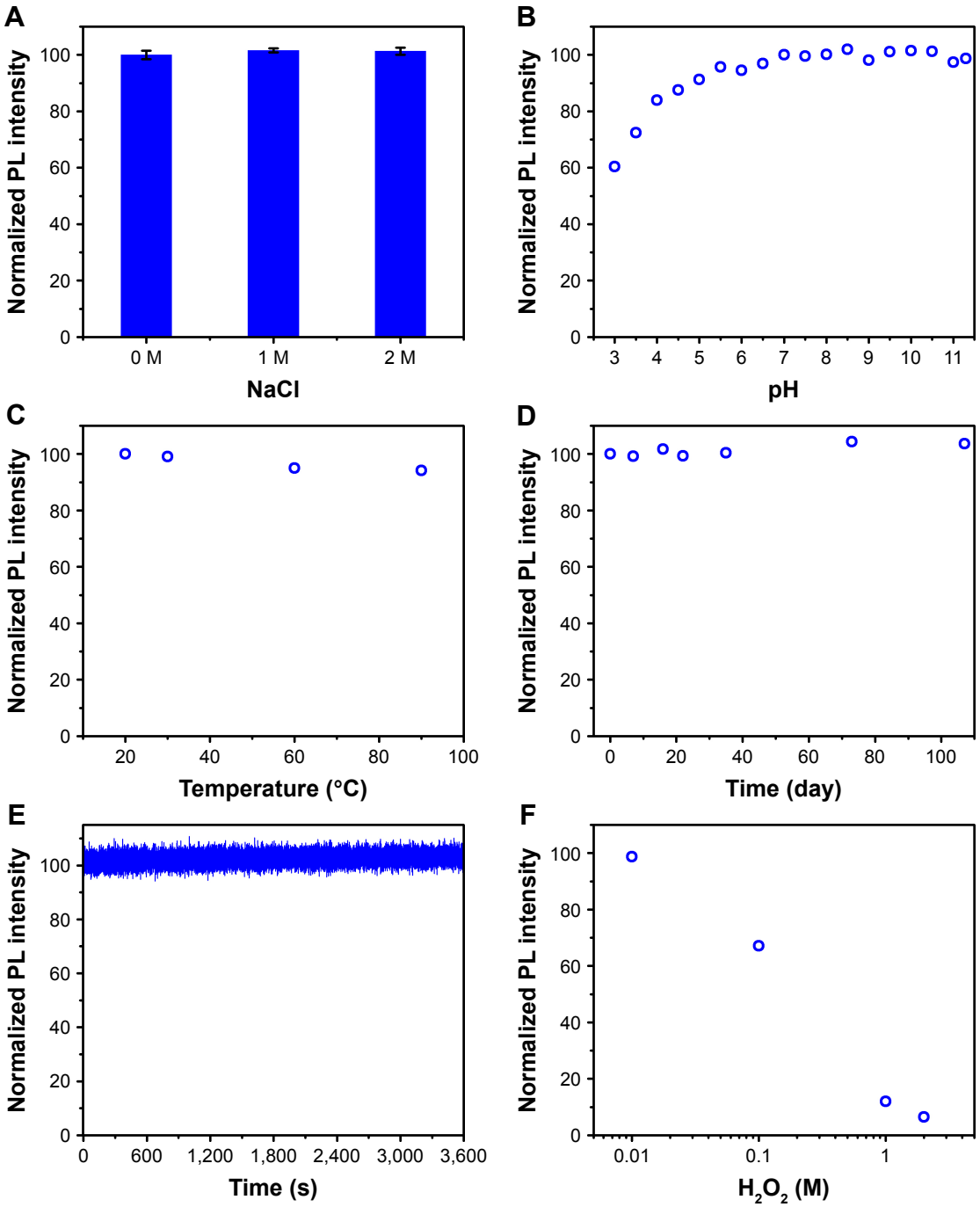

Figure 4 (**A**) Effect of ion strength on the fluorescence intensity of GQDs. (**B**) Effect of pH value on the fluorescence intensity of GQDs. (**C**) Effect of temperature on the fluorescence intensity of GQDs. (**D**) Long-term stability of GQDs at room temperature. (**E**) Fluorescence photostability of GQDs. (**F**) Effect of hydrogen peroxide on the fluorescence intensity of GQDs.

Abbreviations: PL, photoluminescence; GQDs, graphene quantum dots.

Biotoxicity assay and cell imaging

GQDs should show good biocompatibility so that they can be used in bioimaging. The cytotoxicity of as-synthesized GQDs was studied using a standard 3-(4,5-dimethylthiazol-2-yl)-2,5-diphenyltetrazolium bromide (MTT) cell viability assay. HeLa cell viability was evaluated after the cells were exposed to 0–400 μg/mL GQDs for 24 hours. As shown in Figure 5, when the concentration of GQDs increased to 400 μg/mL, the cell survival rate is more than 80%, suggesting that the fluorescent GQDs can serve as an effective biological imaging probe with low cytotoxicity.

To demonstrate the potential application of the GQDs as a fluorescent probe, we performed in vitro cell imaging experiments using a HeLa cell line as a model. After being

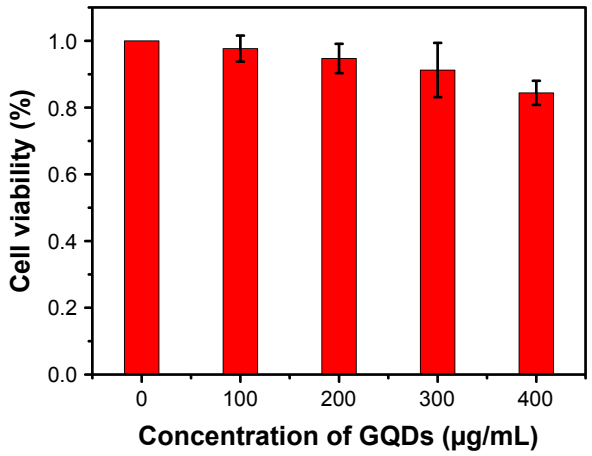

Figure 5 Cell viability of HeLa cancer cells after incubation with GQDs at different concentrations after 24 hours.
Abbreviation: GQDs, graphene quantum dots.

incubated with GQDs (100 μg/mL) for 2 hours, the bright-field and fluorescence images were separately recorded. Figure 6 shows that the cells are lit up brightly by internalized GQDs. Simultaneously, it was noticed that the GQDs were distributed not only in the cytoplasm. The GQDs could penetrate into the nuclei probably due to their ultra-small size (as indicated by the red arrows).[35] Further experiments were conducted to confirm the nuclear penetration of GQDs.

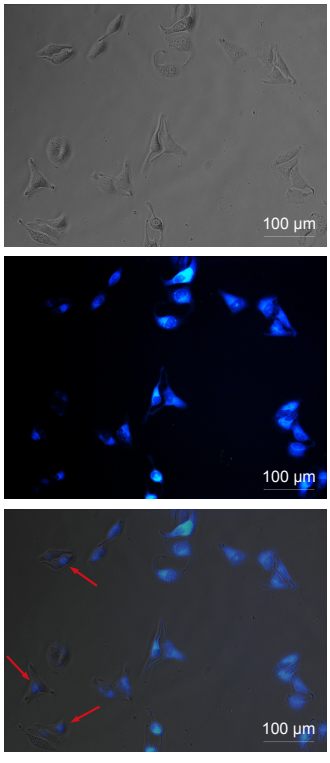

Figure 6 Microscopy images of HeLa cells after incubation with GQDs for 2 hours (from left to right, bright-field image, fluorescence image, and merged image). As indicated by the red arrows, the GQDs can penetrate into the nuclei.
Abbreviation: GQDs, graphene quantum dots.

The nucleus of HeLa cell was stained with acridine orange/ethidium bromide (AO/EB) dyes. It can be seen that the localized blue emission from GQDs and green emission from AO/EB dyes show some overlap (Figure S2). This clearly supports that the blue fluorescent GQDs can enter into the nucleus.

Conclusion

We developed a fast pyrolytic carbonization route to synthesize GQDs using trisodium citrate as precursor. Ultra-small monolayer GQDs (1.3±0.5 nm) with blue-photoluminescence have been obtained via ultrafiltration. The quantum yield of GQDs is measured to be 3.6% with excitation at 330 nm and the average fluorescence lifetime is 2.78 ns. Such GQDs have shown good water solubility, excellent stability, and favorable biocompatibility. The blue fluorescent GQDs have been shown to be effective for bioimaging. It adds a new dimension to the application of graphene materials for nanomedicine.

Acknowledgment

We sincerely acknowledge the financial support of the National Natural Science Foundation of China (81772287), the Program for Innovative leading talents in Fujian Province (2016B016), Joint Project of Major Diseases in Xiamen City of China (3,502Z20179044), and the Natural Science Foundation of Fujian Province (2016J01643).

Disclosure

The authors report no conflicts of interest in this work.

References

1. Bianco A, Cheng H-M, Enoki T, et al. All in the graphene family – a recommended nomenclature for two-dimensional carbon materials. *Carbon*. 2013;65:1–6.
2. Shen J, Zhu Y, Yang X, Zong J, Zhang J, Li C. One-pot hydrothermal synthesis of graphene quantum dots surface-passivated by polyethylene glycol and their photoelectric conversion under near-infrared light. *New J Chem*. 2012;36(1):97–101.
3. Zhang Z, Zhang J, Chen N, Qu L. Graphene quantum dots: an emerging material for energy-related applications and beyond. *Energy Environ Sci*. 2012;5(10):8869–8890.
4. Li L, Wu G, Yang G, Peng J, Zhao J, Zhu JJ. Focusing on luminescent graphene quantum dots: current status and future perspectives. *Nanoscale*. 2013;5(10):4015–4039.
5. Ponomarenko LA, Schedin F, Katsnelson MI, et al. Chaotic Dirac billiard in graphene quantum dots. *Science*. 2008;320(5874):356–358.
6. Ls L, Yan X. Colloidal graphene quantum dots. *J Phys Chem Lett*. 2010;1(17):2572–2576.
7. Jin SH, Kim DH, Jun GH, Hong SH, Jeon S. Tuning the photoluminescence of graphene quantum dots through the charge transfer effect of functional groups. *ACS Nano*. 2013;7(2):1239–1245.
8. Zhu S, Song Y, Wang J, et al. Photoluminescence mechanism in graphene quantum dots: quantum confinement effect and surface/edge state. *Nano Today*. 2017;13:10–14.

9. Roy P, Periasamy AP, Lin CY, et al. Photoluminescent graphene quantum dots for in vivo imaging of apoptotic cells. *Nanoscale*. 2015; 7(6):2504–2510.
10. Zheng XT, Than A, Ananthanaraya A, Kim DH, Chen P. Graphene quantum dots as universal fluorophores and their use in revealing regulated trafficking of insulin receptors in adipocytes. *ACS Nano*. 2013; 7(7):6278–6286.
11. Wu X, Tian F, Wang W, Chen J, Wu M, Zhao JX. Fabrication of highly fluorescent graphene quantum dots using L-glutamic acid for in vitro/in vivo imaging and sensing. *J Mater Chem C Mater*. 2013;1(31): 4676–4684.
12. Sun H, Wu L, Wei W, Qu X, Xg Q. Recent advances in graphene quantum dots for sensing. *Mater Today*. 2013;16(11):433–442.
13. Wang Z, Xia J, Zhou C, et al. Synthesis of strongly green-photoluminescent graphene quantum dots for drug carrier. *Colloids Surf B Biointerfaces*. 2013;112(3):192–196.
14. Han Y, Tang D, Yang Y, et al. Non-metal single/dual doped carbon quantum dots: a general flame synthetic method and electro-catalytic properties. *Nanoscale*. 2015;7(14):5955–5962.
15. Yeh TF, Teng CY, Chen SJ, Teng H. Nitrogen-doped graphene oxide quantum dots as photocatalysts for overall water-splitting under visible light illumination. *Adv Mater*. 2014;26(20):3297–3303.
16. Gupta V, Chaudhary N, Srivastava R, Sharma GD, Bhardwaj R, Chand S. Luminscent graphene quantum dots for organic photovoltaic devices. *J Am Chem Soc*. 2011;133(26):9960–9963.
17. Liu H, Ye T, Mao C. Fluorescent carbon nanoparticles derived from candle soot. *Angew Chem Int Ed Engl*. 2007;46(34):6473–6475.
18. Ye R, Xiang C, Lin J, et al. Coal as an abundant source of graphene quantum dots. *Nat Commun*. 2013;4:2943.
19. Pan D, Zhang J, Li Z, Wu M, Mh W. Hydrothermal route for cutting graphene sheets into blue-luminescent graphene quantum dots. *Adv Mater*. 2010;22(6):734–738.
20. Li L-L, Ji J, Fei R, et al. A facile microwave avenue to electrochemiluminescent two-color graphene quantum dots. *Adv Funct Mater*. 2012;22(14):2971–2979.
21. Shin Y, Lee J, Yang J, et al. Mass production of graphene quantum dots by one-pot synthesis directly from graphite in high yield. *Small*. 2014; 10(5):866–870.
22. Dong Y, Chen C, Zheng X, et al. One-step and high yield simultaneous preparation of single- and multi-layer graphene quantum dots from CX-72 carbon black. *J Mater Chem*. 2012;22(18):8764–8766.
23. Lin L, Zhang S. Creating high yield water soluble luminescent graphene quantum dots via exfoliating and disintegrating carbon nanotubes and graphite flakes. *Chem Commun*. 2012;48(82):10177–10179.
24. Peng J, Gao W, Gupta BK, et al. Graphene quantum dots derived from carbon fibers. *Nano Lett*. 2012;12(2):844–849.
25. Li Y, Hu Y, Zhao Y, et al. An electrochemical avenue to green-luminescent graphene quantum dots as potential electron-acceptors for photovoltaics. *Adv Mater*. 2011;23(6):776–780.
26. Tang L, Ji R, Cao X, et al. Deep ultraviolet photoluminescence of water-soluble self-passivated graphene quantum dots. *ACS Nano*. 2012;6(6):5102–5110.
27. Zhu S, Zhang J, Qiao C, et al. Strongly green-photoluminescent graphene quantum dots for bioimaging applications. *Chem Commun*. 2011;47(24):6858–6860.
28. Dong Y, Shao J, Chen C, et al. Blue luminescent graphene quantum dots and graphene oxide prepared by tuning the carbonization degree of citric acid. *Carbon*. 2012;50(12):4738–4743.
29. Chen G, Zhuo Z, Ni K, et al. Rupturing C60 molecules into graphene-oxide-like quantum dots: structure, photoluminescence, and catalytic application. *Small*. 2015;11(39):5296–5304.
30. Liu R, Wu D, Feng X, Müllen K. Bottom-up fabrication of photoluminescent graphene quantum dots with uniform morphology. *J Am Chem Soc*. 2011;133(39):15221–15223.
31. Schroeder KL, Goreham RV, Nann T. Graphene quantum dots for theranostics and bioimaging. *Pharm Res*. 2016;33(10):2337–2357.
32. Zhuang Q, Wang Y, Ni Y, Yn N. Solid-phase synthesis of graphene quantum dots from the food additive citric acid under microwave irradiation and their use in live-cell imaging. *Lumin*. 2016;31(3):746–753.
33. Gao T, Wang X, Yang LY, et al. Red, yellow, and blue luminescence by graphene quantum dots: syntheses, mechanism, and cellular imaging. *ACS Appl Mater Interfaces*. 2017;9(29):24846–24856.
34. Gokhale R, Singh P. Blue luminescent graphene quantum dots by photochemical stitching of small aromatic molecules: fluorescent nanoprobes in cellular imaging. *Part Part Syst Char*. 2014;31(4):433–438.
35. Wu C, Wang C, Han T, Zhou X, Guo S, Zhang J. Insight into the cellular internalization and cytotoxicity of graphene quantum dots. *Adv Healthc Mater*. 2013;2(12):1613–1619.
36. Kim J, Suh JS. Size-controllable and low-cost fabrication of graphene quantum dots using thermal plasma jet. *ACS Nano*. 2014;8(5): 4190–4196.
37. Bian S, Shen C, Qian Y, Liu J, Xi F, Dong X. Facile synthesis of sulfur-doped graphene quantum dots as fluorescent sensing probes for Ag^+ ions detection. *Sens Actuators B Chem*. 2017;242:231–237.
38. Alizadeh T, Shokri M, Hanifehpour Y, Joo SW, Sang WJ. A new hydrogen cyanide chemiresistor gas sensor based on graphene quantum dots. *Int J Environ Anal Chem*. 2016;96(8):763–775.
39. Wang S, Chen Z-G, Cole I, Li Q. Structural evolution of graphene quantum dots during thermal decomposition of citric acid and the corresponding photoluminescence. *Carbon*. 2015;82:304–313.

Supplementary materials

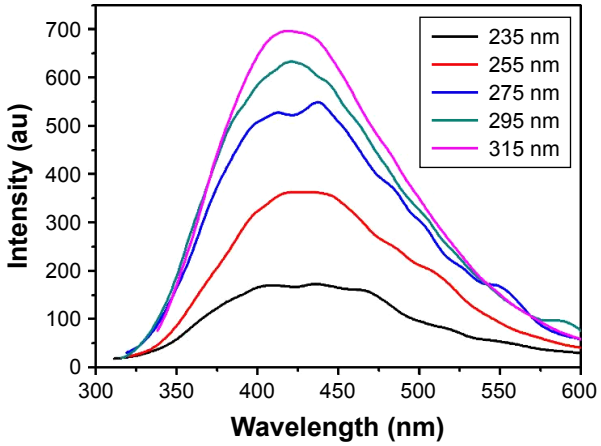

Figure S1 Fluorescence emission spectra of GQDs with different excitation wavelength.
Abbreviation: GQDs, graphene quantum dots.

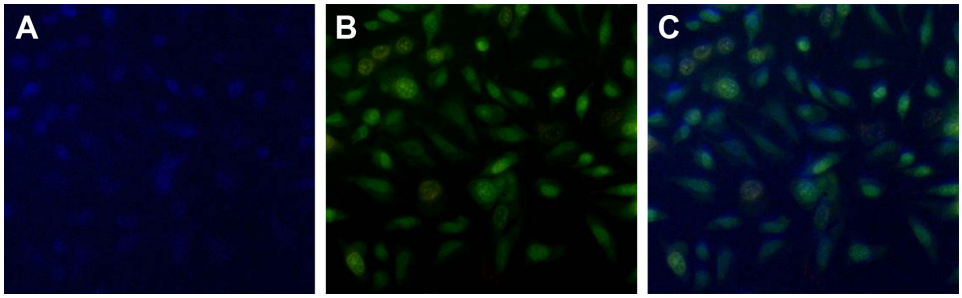

Figure S2 Fluorescent images of HeLa cells (**A**) after treatment with GQDs; (**B**) after staining with AO/EB dyes. (**C**) Merged image of (**A** and **B**).
Abbreviations: GQDs, graphene quantum dots; AO/EB, acridine orange/ethidium bromide.